Original Article

The role of PET imaging probes for early monitoring the response to tamoxifen therapy in a xenograft nude mouse model of ER-positive breast cancer: comparison of ^{18}F-FDG, ^{18}F-FES, and ^{18}F-FLT

Bin Zhang[1], Jiajia Dong[1], Zhenxin Wang[2], Qian Xiong[2], Shengming Deng[1]

Departments of [1]Nuclear Medicine, [2]Oncology, The First Affiliated Hospital of Soochow University, Suzhou, Jiangsu Province, China

Abstract: Aim: In the present study, the possibility of using ^{18}F-fluorodeoxyglucose (^{18}F-FDG), ^{18}F-fluoro-17β-estradiol (^{18}F-FES), and 3'-deoxy-3'-^{18}F-fluorothymidine (^{18}F-FLT) to monitor the response to tamoxifen therapy was assessed as early as 3 days in a mouse xenograft model of estrogen receptor-positive (ER+) breast cancer. Materials and Methods: Nude mice bearing ER+ human breast cancer MCF-7 xenografts were treated with vehicle or tamoxifen. Micro-PET imaging with ^{18}F-FDG, ^{18}F-FLT, and ^{18}F-FES was performed prior to and 3 days after treatment. Histopathologic analyses, including hematoxylin and eosin staining (H&E) and immunohistochemical studies (ERα, ERβ, GLUT1, Ki-67, and PCNA), were performed. Results: ^{18}F-FLT and ^{18}F-FES uptake was decreased on day 3 after tamoxifen treatment (P < 0.05), while ^{18}F-FDG uptake showed no significant decrease (P > 0.05). Immunohistochemical analysis of tumor samples indicated that staining of ERα, GLUT1, Ki-67, and PCNA was decreased in the tamoxifen-treated group compared with the vehicle-treated group (P < 0.05). However, no notice-able difference of ERβ staining was observed in tumor cells between vehicle-treated and tamoxifen-treated groups (P = 0.471). Peri-necrotic GLUT1 expression was particularly apparent near the necrotic area of tamoxifen-treated tumors. Conclusion: ^{18}F-FES and ^{18}F-FLT are superior to ^{18}F-FDG as PET imaging probes for monitoring the response to tamoxifen treatment as early as 3 days in ER+ breast cancer. Peri-necrotic GLUT1 expression might be one of the reasons why ^{18}F-FDG PET could not early evaluate the response to tamoxifen therapy. ^{18}F-FES PET could reliably assess down-regulation of ERα caused by tamoxifen treatment.

Keywords: ^{18}F-FES, ^{18}F-FLT, ^{18}F-FDG, tamoxifen, breast cancer, response evaluation

Introduction

As the most common malignant tumor in females, breast cancer alone accounts for 30% all newly diagnosed cancer cases among women in USA [1]. Hormone receptor positive (HR+), defined as either estrogen receptor-positive (ER+) and/or progesterone receptor-positive (PR+) tumors account for approximately 70-80% of breast cancers [2].

Endocrine therapy remains one of the mainstream treatments for selected patients with ER+ breast cancer. Tamoxifen, as an estrogen modulator, has been widely used in the treatment of ER+ breast cancer since 1977. Although the clinical benefit of tamoxifen is prominent, many patients with ER+ breast cancer have experienced resistance or other adverse side effects following the tamoxifen therapy. Therefore, it is urgently necessary to develop accurate methodologies for an early evaluation of response at an early time point, by which patients without good response can be switched to more effective alternative treatments early during the course of tamoxifen administration.

In recent decades, positron emission tomography (PET) has become the main technique for molecular imaging. PET permits non-invasive visualization and quantification of various biological processes, which are modulated during therapy of breast cancer, including metabolism, receptor density, cell proliferation, and up-

take of therapeutic agents [3]. ^{18}F-fluorodeoxyglucose (^{18}F-FDG) is the most widely used radiotracer for diagnosis, staging, and post-treatment evaluation of cancer. However, ^{18}F-FDG is not strictly tumor-specific, and false-positive results may arise secondary to uptake in inflammatory cells and granulation tissue [4]. ^{18}F-fluoro-17β-estradiol (^{18}F-FES) is emerging as a specific ER-targeted molecular probe for evaluation of ER expression in breast cancer. Some studies have shown that ^{18}F-FES PET can be used to detect ER+ breast cancer lesions and monitor treatment response [5, 6]. 3'-Deoxy-3'-^{18}F-fluorothymidine (^{18}F-FLT) is another PET tracer which reflects proliferative activity in cancer lesions. ^{18}F-FLT crosses the cell membrane and becomes phosphorylated by thymidine kinase 1 (TK-1) into a highly charged product, which is intracellularly trapped and can be imaged using PET. In addition, some studies have reported that ^{18}F-FLT PET imaging can be used to evaluate response to treatment in patients with cancer [7, 8]. It remains unclear which type of radiotracers can be used to monitor the early response to tamoxifen treatment in ER+ breast cancer. Therefore, the goal of this study was to assess the possibility of using ^{18}F-FDG, ^{18}F-FES, and ^{18}F-FLT to monitor the response to tamoxifen treatment as early as 3 days in breast cancer with a mouse xenograft model of ER+ breast cancer. Additionally, immunohistochemical (IHC) analyses of ERα, ERβ, glucose transporter type 1 (GLUT1), Ki-67, and proliferating cell nuclear antigen (PCNA) were performed to investigate the relationship between the underlying biology and the imaging parameters.

Materials and methods

Cell culture

The human breast cancer cell line MCF-7 was purchased from the Shanghai Cell Bank of the Chinese Academy of Science. Cells were cultured in RPMI 1640 medium (Gibco, Rockville, MD, USA) supplemented with 10% heat-inactivated fetal bovine serum (FBS, Gibco, Rockville, MD, USA) and 1% penicillin/streptomycin at 37°C in a humidified atmosphere containing 5% CO_2.

Animal tumor model

Female athymic nude mice (age, 3-4 weeks) were purchased from the Shanghai Experimental Animal Center (Shanghai, China) and bred in filter-top cages under specific pathogen-free conditions. The MCF-7 model was established through subcutaneous injections of 1×10^7 cells in 200 μL of phosphate-buffered saline (PBS) into the subcutaneous tissue of the right axillary fossa. Mice were subcutaneously injected with 0.2 mL 17β-estradiol (0.15 mg/mL) around the tumor once daily to promote the tumor growth. Tumor volumes were estimated using the formula as follows: $0.5 \times length \times width^2$. Tamoxifen was administered when the tumor volume reached~50 mm^3 (3-4 weeks after inoculation).

The mice were randomly and evenly assigned into four groups (n = 5 per group). Mice were treated with vehicle (ethanol in normal saline) in the control group. Within the groups receiving tamoxifen treatment, an oral dose of 0.2 mg tamoxifen (Sigma) was intra-gastrically administrated once daily for 3 days.

This study was carried out in accordance with the guidelines of the Institutional Animal Care and Use Committee at the First Affiliated Hospital of Soochow University, and animal-related protocols were approved by the Animal Ethics Committee of the First Affiliated Hospital of Soochow University.

Micro-PET imaging and quantitative analysis

Micro-PET scans and image analysis were performed on day 0 prior to the treatment (baseline) and day 3 after treatment using an Inveon micro-PET scanner (Siemens Medical Solutions).

MCF-7 tumor-bearing mice were injected with 3.7 MBq (100 μCi) of ^{18}F-FDG, ^{18}F-FES, or ^{18}F-FLT via tail vein under isoflurane-induced anesthesia. For ^{18}F-FDG scans, mice were fasted for 8 hours before tracer injection. Subsequently, 20-minute static scans were acquired at 1 hour after injection. During the scanning period, mice were maintained under isoflurane-induced anesthesia and positioned in the center PET ring field of view.

The images were reconstructed using the 2-dimensional ordered subset expectation maximization (OSEM) algorithm, and no attenuation correction was applied. Regions of interest (ROIs) were drawn over the tumor using ASI Pro

VMTM software (Siemens Medical Solutions USA Inc. Knoxville, TN, USA) on decay-corrected whole-body coronal images. Quantitative data are expressed as SUV_{max}, which was defined as maximal volumic activity in the tumor (MBq/mL)/injected dose (MBq)/the body weight (g). Changes after therapy are described as $\Delta SUV_{max} = (SUV_{max}$ day 3-SUV_{max} day 0)/SUV_{max} day 0 × 100%.

Histological and IHC analyses

Tumor tissue samples from tumor-bearing mice treated with tamoxifen or vehicle were excised, fixed in 10% formalin and paraffin embedded. Then paraffin-embedded tissues were cut into 4-μm sections and stained with hematoxylin and eosin (H&E) or subjected to IHC analysis for ERα, ERβ, GLUT1, Ki-67, and PCNA. Antibodies used in the present study included anti-ERα, anti-ERβ (Abcam, Shanghai, China, dilution 1:100), anti-Ki-67, anti-PCNA (Gene Tech, Shanghai, China, dilution 1:100) and anti-GLUT1 (Sigma-Aldrich, Shanghai, China, dilution 1:50).

According to the IHC procedures, tumor specimens were subsequently subjected to stepwise hydration, followed by blockage with 3% H_2O_2 for endogenous peroxidase and antigen recovery with Tris-buffered saline (TBS). FBS and antibodies, biotinylated secondary antibody, horseradish peroxidase-labeled avidin streptomycin, and diaminobenzidine staining were sequentially added to tumor specimens. Finally, the stained specimens were counterstained with hematoxylin and dehydrated.

H&E images were analyzed in representative sections of the tumor to evaluate the tumor morphology and the extent of viable tumor. Cells stained in both the cytoplasm and nucleus were regarded as the viable tumor cells, whereas cells stained with eosin only or no staining were regarded as apoptotic/necrotic areas.

Expression of ERα, ERβ, GLUT1, Ki-67, and PCNA were determined by two independent experienced pathologists unaware of micro-PET information. Specimens were scanned in low-power fields to determine several representative areas. High-power fields (× 400) were used for cell counting. At least five representative fields with total cell number of 500 were observed to count the positive cells.

A semi-quantitative method was used for scoring ERα+ and ERβ+ areas as described by Peng J et al. [9]. The classes of 0-5%, 5-25%, 25-50%, 50-75%, and > 75% positively stained cells were assigned semi-quantitative scores of 0, 1, 2, 3, and 4, respectively. The intensity was scored according to the following criteria: (0) negative staining; (1) weak staining; (2) moderate staining; and (3) strong staining. The final IHC score was generated by multiplying the staining intensity score by the percentage score.

It was impossible to quantify GLUT1 immunostaining by grading the proportion of cells because staining of the tumor was diffuse in most specimens. Therefore, GLUT1 was scored according to intensity only.

IHC staining for Ki-67 and PCNA was performed to evaluate the proliferation of tumor cells. The brownish nuclei were selected, and the number of Ki-67+ and PCNA+ tumor cells was counted. The immunosignal index was calculated by dividing the number of positively stained cells by the number of whole tumor cells.

Statistical analysis

Quantitative data are expressed as mean ± standard deviation (SD). Student's t-test (two-tailed) was applied to determine statistical significance between experimental and control groups using IBM SPSS 19.0 software (SPSS Inc. Chicago, IL, USA). *P* values < 0.05 were considered as statistically significant.

Results

Micro-PET images

When initial micro-PET imaging was performed, the average tumor volume reached 60.06 ± 4.39 mm³. **Figure 1A** illustrates that significant uptake was clearly visualized in tumors as well as in bladders in the case of all micro-PET tracers. ^{18}F-FDG showed physiologically high uptake in the heart and brain. No statistically significant difference of ^{18}F-FDG uptake was observed between day 3 after tamoxifen treatment and baseline, with the SUV_{max} of 1.12 ± 0.16 and 1.05 ± 0.11, respectively (P = 0.378).

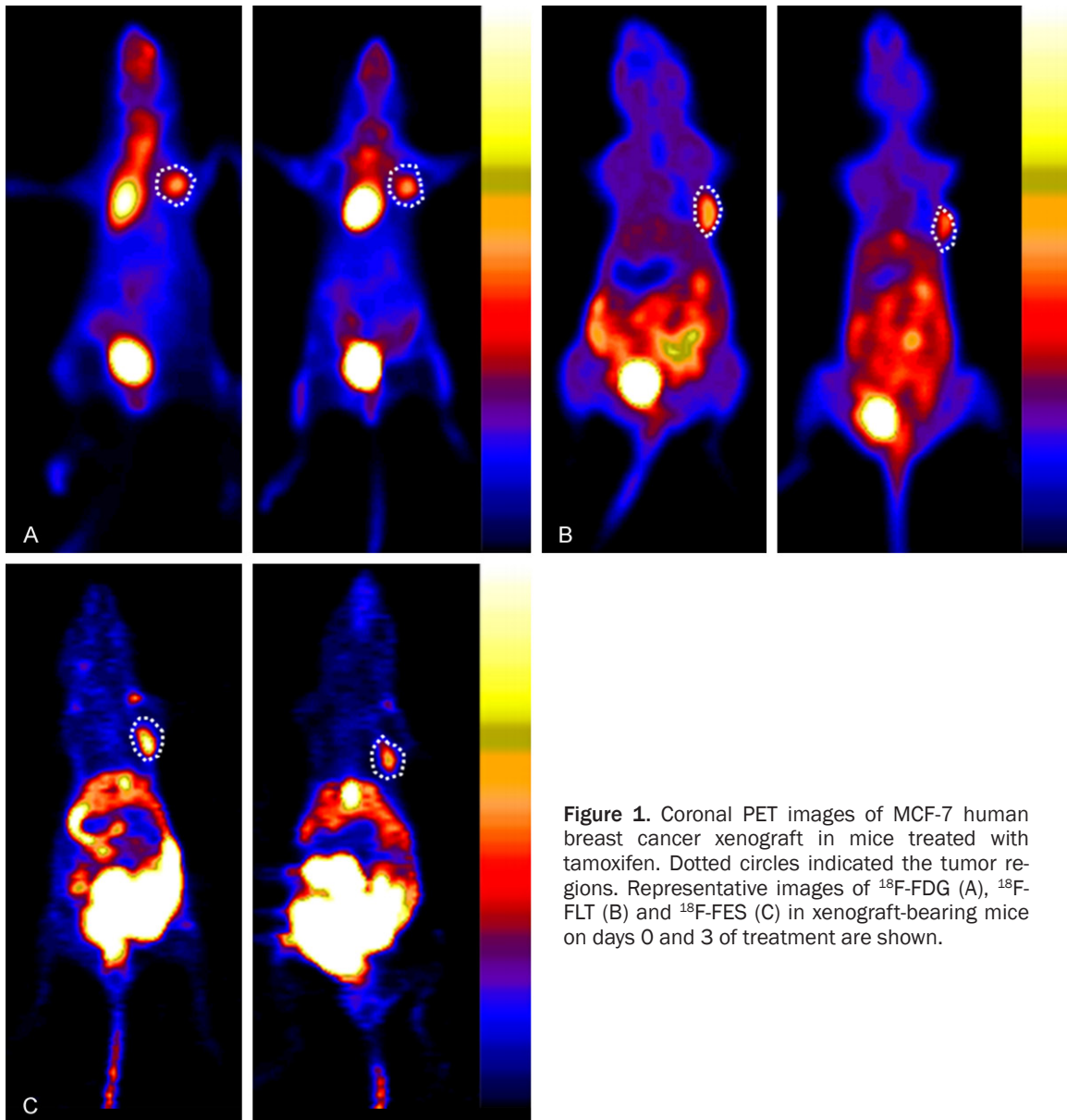The tumor lesion had a good uptake of ^{18}F-FLT. Significant uptake of ^{18}F-FLT was also visual-

Figure 1. Coronal PET images of MCF-7 human breast cancer xenograft in mice treated with tamoxifen. Dotted circles indicated the tumor regions. Representative images of ^{18}F-FDG (A), ^{18}F-FLT (B) and ^{18}F-FES (C) in xenograft-bearing mice on days 0 and 3 of treatment are shown.
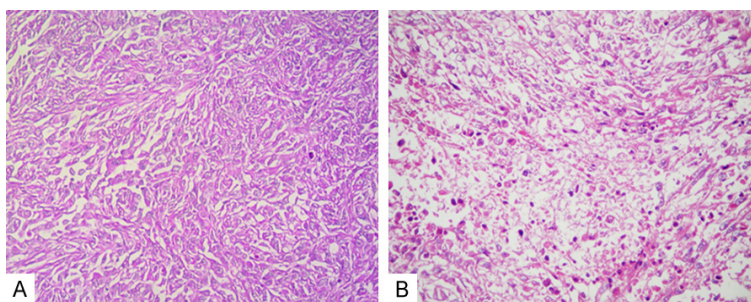

Figure 2. Histopathologic specimens with H&E staining. Microscope images (magnification × 200) of the vehicle-treated (A) and tamoxifen-treated (B) groups are shown.

ized in the kidney, spleen and intestine. Quantitative image analysis showed notable differences (ΔSUV_{max} = 0.13 ± 0.11) between the ^{18}F-FLT uptake of the pre-therapeutic tumors (SUV_{max} = 0.85 ± 0.09) and the tamoxifen-treated tumors (SUV_{max} = 0.72 ± 0.08, P = 0.039, **Figure 1B**).

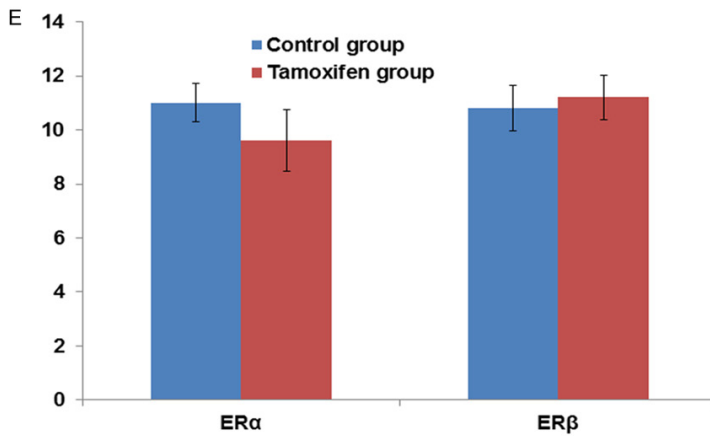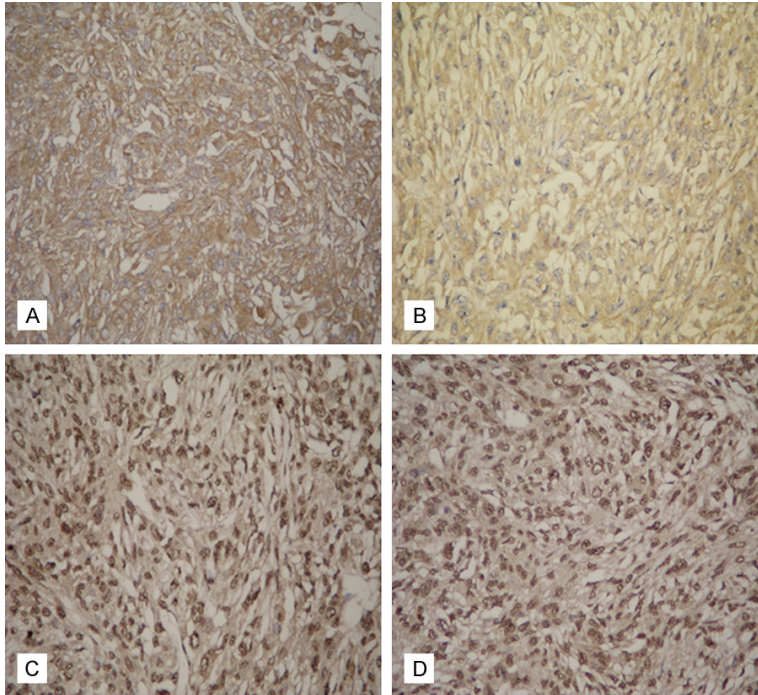High ^{18}F-FES uptake was visualized in tumors as well as the

Figure 3. Immunostaining of ERα and ERβ in tumor samples acquired from experimental animals bearing MCF-7 xenografts. Expression of ERα in the vehicle-treated (A) and tamoxifen-treated (B) groups. Representative IHC staining of ERβ in vehicle-treated (C) and tamoxifen-treated (D) groups. Magnification × 200. Expression of ERα and ERβ for the vehicle-treated and tamoxifen-treated groups (E) are summarized. Significant difference of ERα expression was found between tamoxifen-treated and vehicle-treated groups (P < 0.05). No noticeable difference of ERβ staining was observed between vehicle-treated and tamoxifen-treated groups (P > 0.05). *Columns*, mean; *bars*, SE.

Histopathologic findings

Different characteristics of tumor apoptosis/necrosis were observed between the two groups by H&E staining of tumor specimens (**Figure 2**). Actively mitotic tumor cells were abundant in the vehicle-treated group, whereas they were sparse in the tamoxifen group. Moreover, H&E staining indicated that extensive areas of tumor necrosis were present in tamoxifen-treated mice.

IHC analysis

Cytoplasmic immunoreaction of ERα and nuclear immunoreaction of ERβ were detected in tumor cells. IHC analysis revealed a significantly lower IHC score of ERα in the treatment group compared with the control group (9.60 ± 1.14 *vs.* 11.00 ± 0.71, respectively; P = 0.048). However, no noticeable difference of ERβ staining was observed in tumor cells between vehicle-treated and tamoxifen-treated groups (10.80 ± 0.84 *vs.* 11.20 ± 0.84, respectively; P = 0.471) (**Figure 3**).

For GLUT1, a very diffuse staining of the entire tumor cell was observed. Moreover, a statistically significant difference in the IHC score of GLUT1 between the vehicle-treated group and the tamoxifen-treated group (2.72 ± 0.16 *vs.* 2.48 ± 0.13, respectively; P = 0.034) was observed. Furthermore, peri-necrotic GLUT1 expression was particularly apparent near the necrotic area of tamoxifen-treated tumors (**Figure 4**).

Immunostaining for Ki67 and PCNA was present at the nuclear level. Microscopic examination of tumor xenograft sections showed a decreased immunoreactivity for Ki67 (19.60 ± 1.82 *vs.* 26.20 ± 2.59, respectively; P = 0.002)

gallbladder and bowel, which was consistent with hepatobiliary excretion of ^{18}F-FES. Quantification radioactivity analysis showed a significantly decreased ^{18}F-FES uptake (ΔSUV$_{max}$ = 0.32 ± 0.03) in the MCF-7 xenograft after the treatment (SUV$_{max}$ = 0.32 ± 0.09) compared with baseline ^{18}F-FES uptake (SUV$_{max}$ = 0.64 ± 0.12, P = 0.006, **Figure 1C**).
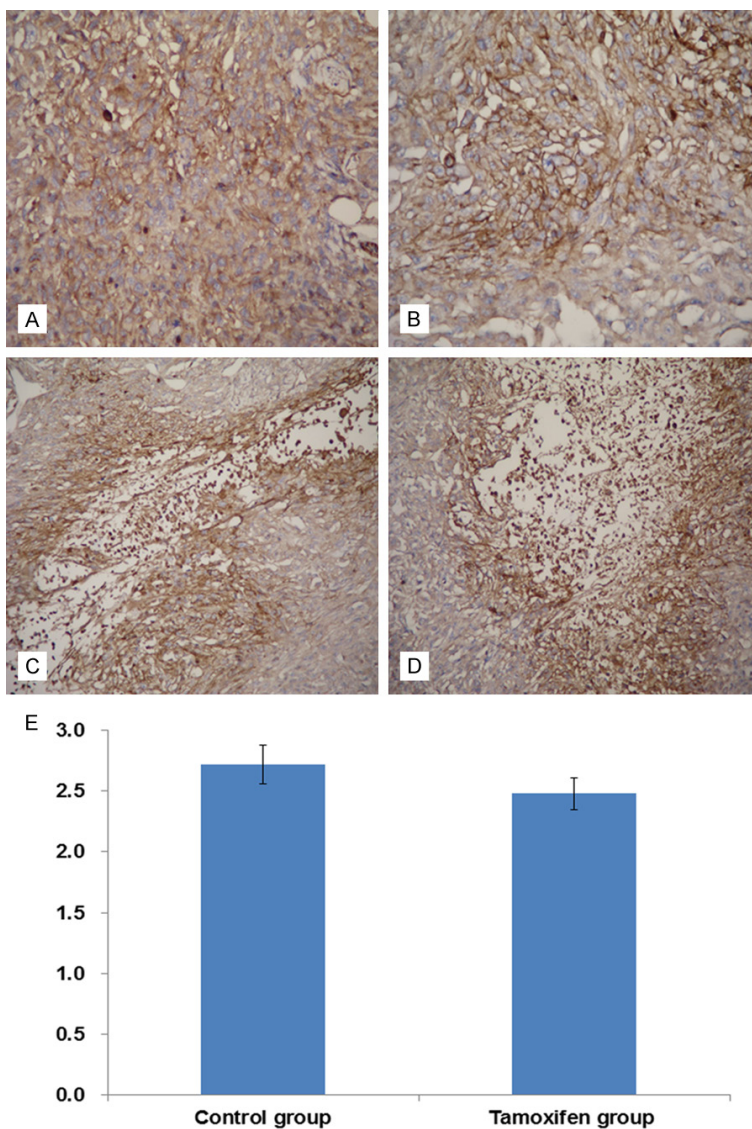
Figure 4. IHC staining of GLUT1 expression in representative tumor sections. Staining for GLUT1 in tumors is shown for the vehicle-treated group (A) and the tamoxifen-treated group (B). Magnification × 200. GLUT1 expression also appeared in peri-necrotic areas near tamoxifen-treated tumors (C and D). Magnification × 20. Expression of GLUT1 for the vehicle-treated and tamoxifen-treated groups (E) is summarized. A significant difference of GLUT1 expression was found between tamoxifen-treated and vehicle-treated groups (P < 0.05). *Columns,* mean; *bars,* SE.

ance of effective therapy in patients with responsive tumors or avoids the use of expensive, toxic and ineffective treatment in those patients with unresponsive tumors. Recently, an increasing number of studies have reported the utilization of PET in the treatment evaluation of different cancers at very early time points [10-12]. According to these results, the best radiotracer and timing for early evaluation may depend on the drugs used and the type of disease [13]. Several investigators have recently used PET to evaluate treatment response of breast cancer in animal models. However, in those studies PET is performed at later times than our study. Moreover, no MCF-7 cell line or tamoxifen has been used, no different radiotracers have been compared, and no comprehensive IHC examination of ERα, ERβ, GLUT1, Ki-67, and PCNA has been performed [14-17]. To the best of our knowledge, this is the first study to have evaluated the efficiency of ^{18}F-FDG, ^{18}F-FES, and ^{18}F-FLT in monitoring the response to tamoxifen treatment as early as 3 days in an animal model of breast cancer.

In this study, it was impossible to assess the therapy efficacy with ^{18}F-FDG in the early phase because there was no significant difference in ^{18}F-FDG up-

and PCNA (61.40 ± 3.91 *vs.* 70.80 ± 5.26, respectively; P = 0.013) in the tamoxifen-treated group compared with the vehicle-treated group (**Figure 5**).

Discussion

In clinical settings, early response monitoring would greatly benefit management of patients receiving treatment, which assures continu-

take by breast tumor between the tamoxifen-treated and vehicle-treated groups on day 3. As a glucose analogue, ^{18}F-FDG enters tumor cells via glucose transporters. Among these glucose transporters, GLUT1 is considered to largely determine ^{18}F-FDG uptake in cancer [18]. However, there is a controversy surrounding the correlation between GLUT1 and ^{18}F-FDG in breast cancer. In some studies [19, 20], strong correlation between GLUT1 and ^{18}F-FDG
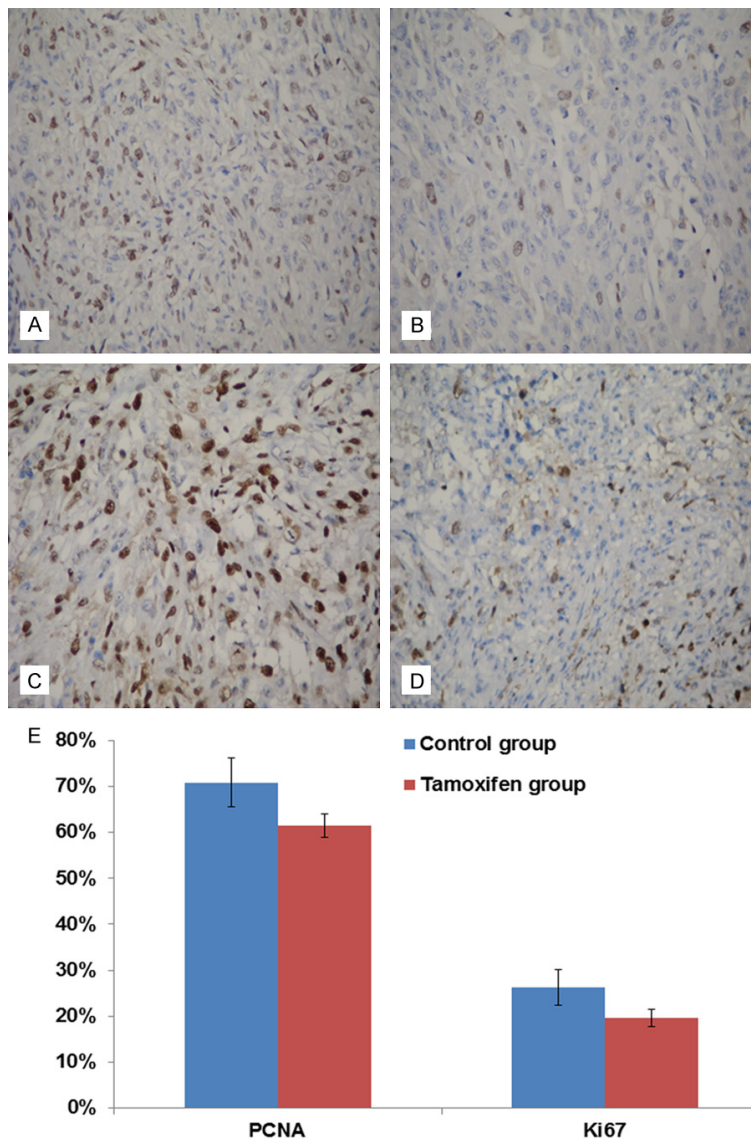
Figure 5. Tumor cell proliferation in representative tumor sections. Ki-67+ cells in tumors are shown for the vehicle-treated group (A) and tamoxifen-treated group (B). Typical PCNA-stained histological sections of vehicle-treated tumor (C) and tamoxifen-treated tumor (D) are shown. Magnification × 200. Immunostaining for Ki67 and PCNA in the vehicle-treated and tamoxifen-treated groups (E) is shown. Significant differences of immunostaining for Ki67 and PCNA were found between tamoxifen-treated and vehicle-treated groups (P < 0.05). *Columns,* mean; *bars*, SE.

which was in accordance with some previous reports [23, 24]. This might contribute to the mismatch of changes of 18F-FDG uptake and GLUT1 expression in breast cancer. Aliaga et al. [25] have also observed that the uptake of 18F-FDG in ER+ breast cancer can significantly vary within the first 2 weeks after the initiation of the therapy, and the eventual response can be underestimated or overestimated using 18F-FDG. Therefore, the underlying mechanism should be further investigated.

18F-FLT PET has often been studied in the detection of early biological response following anticancer treatment in a wide range of cancers, including breast cancer, in an animal model [26-28]. In general, these studies have indicated that 18F-FLT PET is sensitive to early molecular changes in xenografts. In line with these studies, our findings suggested that 18F-FLT PET could detect a significant change as early as 3 days after tamoxifen treatment. 18F-FLT has been proposed as an imaging biomarker of proliferation because it is phosphorylated by TK-1 and then trapped inside the cell by entering the thymidine salvage pathway of DNA synthesis without incorporation into the DNA molecule. PCNA is an auxiliary protein necessary for DNA synthesis.

uptake has been noted, whereas such association is not found in other studies [21, 22]. Here, different trends were observed in changes of 18F-FDG uptake and GLUT1 expression in breast cancer, where the GLUT1 expression was more significantly decreased than 18F-FDG uptake in the tamoxifen-treated group. Interestingly, peri-necrotic GLUT1 expression was observed near the necrotic areas of tamoxifen-treated tumors, As PCNA expression is well correlated with DNA synthesis, it has been extensively used as a marker for evaluation of cell proliferation. As a human nuclear protein, the Ki-67 antigen is expressed only in the proliferative phase of the cell cycle, and it is therefore considered to be a reliable proliferative marker. This study assessed expression of both Ki-67 and PCNA to explore the correlation between 18F-FLT

uptake and cell proliferation. Expression of both Ki-67 and PCNA showed a similar decreasing trend with ^{18}F-FLT uptake in tamoxifen-treated tumors. Other investigators have similarly shown such good correlation between ^{18}F-FLT uptake and expression of Ki-67 and PCNA [29, 30].

In recent years, ^{18}F-FES has emerged as a promising predictive biomarker to help identify patients who are likely to benefit from endocrine therapy since its uptake is strongly correlated with the ER expression [31]. However, there are only a few studies about early monitoring of the response to endocrine therapy in breast cancer [15, 32]. In these studies, significant changes in ^{18}F-FES SUV have been found early after endocrine therapy, which is comparable with our findings. Moreover, our data show that ^{18}F-FES is superior to ^{18}F-FLT and ^{18}F-FDG as a PET imaging probe in early evaluation of response to tamoxifen therapy in ER+ breast cancer since ^{18}F-FES uptake exhibited a more significant decrease in the tamoxifen-treated group on day 3 after treatment.

IHC analysis was also performed for ERα and ERβ to explore the relationship between ^{18}F-FES uptake and ER expression. ERα has been extensively studied as a binding target for both diagnostic and therapeutic agents, while the role of ERβ is not fully understood and has not yet been investigated in clinical trials of breast cancer treatment [32]. IHC analysis revealed a significantly decreased ERα expression in the tamoxifen-treated group. However, no noticeable difference of ERβ staining was observed in tumor cells between vehicle-treated and tamoxifen-treated groups. As is known, ^{18}F-FES selectively binds to ERα, and its affinity for ERα is 6.3 times higher than that for ERβ. Moreover, ERα is a well-known target for endocrine therapy with the selective ER modulator tamoxifen [33]. Therefore, this study confirmed that ^{18}F-FES could be used for early and precise evaluation of the efficacy of tamoxifen in a xenograft nude mouse model of ER+ breast cancer.

However, there are some potential limitations in our present study. First, observation was only performed at one time point. It was possible that changes in uptake of radiotracers were missed. A regular time point (day 3) was selected in this study since such time point is widely adopted and early enough for clinical decisions. Second, only one model of breast cancer and one cell line were used in the present study. Therefore, it is necessary to validate these findings through a prospective clinical trial in the future.

Conclusions

^{18}F-FES and ^{18}F-FLT are superior to ^{18}F-FDG as PET imaging probes for monitoring the response to tamoxifen treatment as early as 3 days in ER+ breast cancer. Peri-necrotic GLUT1 expression might be one of the reasons why ^{18}F-FDG PET could not early evaluate the response to tamoxifen therapy. Collectively, ^{18}F-FES PET could reliably assess the tamoxifen-induced down-regulation of ERα.

Acknowledgements

Disclosure of conflict of interest

None.

Address correspondence to: Shengming Deng, Department of Nuclear Medicine, The First Affiliated Hospital of Soochow University, No. 188, Shizi Street, Gusu District, Suzhou 215006, Jiangsu Province, China. Tel: +86-15051510189; E-mail: dshming@163.com

References

[1] Siegel RL, Miller KD, Jemal A. Cancer statistics, 2018. CA Cancer J Clin 2018; 68: 7-30.

[2] Sandoval C, Rahal R, Forte T, Klein-Geltink J, He D, Bryant H. Indicator measures er/pr and her2 testing among women with invasive breast cancer. Curr Oncol 2013; 20: 62-63.

[3] Humbert O, Cochet A, Coudert B, Berriolo-Riedinger A, Kanoun S, Brunotte F, Fumoleau P. Role of positron emission tomography for the monitoring of response to therapy in breast cancer. Oncologist 2015; 20: 94-104.

[4] Kazama T, Faria SC, Varavithya V, Phongkitkarun S, Ito H, Macapinlac HA. FDG PET in the evaluation of treatment for lymphoma: clinical usefulness and pitfalls. Radiographics 2005; 25: 191-207.

[5] Gemignani ML, Patil S, Seshan VE, Sampson M, Humm JL, Lewis JS, Brogi E, Larson SM, Morrow M, Pandit-Taskar N. Feasibility and predictability of perioperative PET and estrogen receptor ligand in patients with invasive breast cancer. J Nucl Med 2013; 54: 1697-1702.

[6] Chae SY, Kim SB, Ahn SH, Kim HO, Yoon DH, Ahn JH, Jung KH, Han S, Oh SJ, Lee SJ, Kim HJ, Son BH, Gong G, Lee HS, Moon DH. A randomized feasibility study of ^{18}F-Fluoroestradiol PET to predict pathologic response to neoadjuvant therapy in estrogen receptor-rich postmenopausal breast cancer. J Nucl Med 2017; 58: 563-568.

[7] Han EJ, Lee BH, Kim JA, Park YH, Choi WH. Early assessment of response to induction therapy in acute myeloid leukemia using ^{18}F-FLT PET/CT. EJNMMI Res 2017; 7: 75.

[8] Crippa F, Agresti R, Sandri M, Mariani G, Padovano B, Alessi A, Bianchi G, Bombardieri E, Maugeri I, Rampa M, Carcangiu ML, Trecate G, Pascali C, Bogni A, Martelli G, de Braud F. ^{18}F-FLT PET/CT as an imaging tool for early prediction of pathological response in patients with locally advanced breast cancer treated with neoadjuvant chemotherapy: a pilot study. Eur J Nucl Med Mol Imaging 2015; 42: 818-830.

[9] Peng J, Ou Q, Wu X, Zhang R, Zhao Q, Jiang W, Lu Z, Wan D, Pan Z, Fang Y. Expression of voltage-gated sodium channel Nav1.5 in non-metastatic colon cancer and its associations with estrogen receptor (ER)-β expression and clinical outcomes. Chin J Cancer 2017; 36: 89.

[10] Geven EJ, Evers S, Nayak TK, Bergström M, Su F, Gerrits D, Franssen GM, Boerman OC. Therapy response monitoring of the early effects of a new BRAF inhibitor on melanoma xenograft in mice: evaluation of (18) F-FDG-PET and (18) F-FLT-PET. Contrast Media Mol Imaging 2015; 10: 203-210.

[11] Song SL, Deng C, Wen LF, Liu JJ, Wang H, Feng D, Wong CY, Huang G. ^{18}F-FDG PET/CT-related metabolic parameters and their value in early prediction of chemotherapy response in a VX2 tumor model. Nucl Med Biol 2010; 37: 327-333.

[12] Aide N, Poulain L, Briand M, Dutoit S, Allouche S, Labiche A, Ngo-Van Do A, Nataf V, Batalla A, Gauduchon P, Talbot JN, Montravers F. Early evaluation of the effects of chemotherapy with longitudinal FDG small-animal PET in human testicular cancer xenografts: early flare response does not reflect refractory disease. Eur J Nucl Med Mol Imaging 2009; 36: 396-405.

[13] Takeuchi S, Zhao S, Kuge Y, Zhao Y, Nishijima K, Hatano T, Shimizu Y, Kinoshita I, Tamaki N, Dosaka-Akita H. ^{18}F-fluorothymidine PET/CT as an early predictor of tumor response to treatment with cetuximab in human lung cancer xenografts. Oncol Rep 2011; 26: 725-730.

[14] Prignon A, Nataf V, Provost C, Cagnolini A, Montravers F, Gruaz-Guyon A, Lantry LE, Talbot JN, Nunn AD. (68) Ga-AMBA and (18) F-FDG f or preclinical PET imaging of breast cancer: effect of tamoxifen treatment on tracer uptake by tumor. Nucl Med Biol 2015; 42: 92-98.

[15] He S, Wang M, Yang Z, Zhang J, Zhang Y, Luo J, Zhang Y. Comparison of ^{18}F-FES, ^{18}F-FDG, and ^{18}F-FMISO PET imaging probes for early prediction and monitoring of response to endocrine therapy in a mouse xenograft model of er-positive breast cancer. PLoS One 2016; 11: e0159916.

[16] Kristian A, Holtedahl JE, Torheim T, Futsaether C, Hernes E, Engebraaten O, Mælandsmo GM, Malinen E. Dynamic 2-Deoxy-2-[18F] Fluoro-D-Glucose positron emission tomography for chemotherapy response monitoring of breast cancer xenografts. Mol Imaging Biol 2017; 19: 271-279.

[17] Chen M, Zhang W, Yuan K, Bo M, Chen B, Li L, Ma Q, Zhu L, Gao S. Preclinical evaluation and monitoring of the therapeutic response of a dual targeted hyaluronic acid nanodrug. Contrast Media Mol Imaging 2017; 2017: 4972701.

[18] Song YS, Lee WW, Chung JH, Park SY, Kim YK, Kim SE. Correlation between FDG uptake and glucose transporter type 1 expression in neuroendocrine tumors of the lung. Lung Cancer 2008; 61: 54-60.

[19] Brown RS, Leung JY, Fisher SJ, Frey KA, Ethier SP, Wahl RL. Intratumoral distribution of tritiated-FDG in breast carcinoma: correlation between Glut-1 expression and FDG uptake. J Nucl Med 1996; 37: 1042-1047.

[20] Bos R, van Der Hoeven JJ, van Der Wall E, van Der Groep P, van Diest PJ, Comans EF, Joshi U, Semenza GL, Hoekstra OS, Lammertsma AA, Molthoff CF. Biologic correlates of (18) fluorodeoxyglucose uptake in human breast cancer measured by positron emission tomography. J Clin Oncol 2002; 20: 379-387.

[21] Groves AM, Shastry M, Rodriguez-Justo M, Malhotra A, Endozo R, Davidson T, Kelleher T, Miles KA, Ell PJ, Keshtgar MR. ^{18}F-FDG PET and biomarkers for tumour angiogenesis in early breast cancer. Eur J Nucl Med Mol Imaging 2011; 38: 46-52.

[22] Avril N, Menzel M, Dose J, Schelling M, Weber W, Jänicke F, Nathrath W, Schwaiger M. Glucose metabolism of breast cancer assessed by ^{18}F-FDG PET: histologic and immunohistochemical tissue analysis. J Nucl Med 2001; 42: 9-16.

[23] Kubo Y, Aishima S, Tanaka Y, Shindo K, Mizuuchi Y, Abe K, Shirabe K, Maehara Y, Honda

H, Oda Y. Different expression of glucose transporters in the progression of intrahepatic cholangiocarcinoma. Hum Pathol 2014; 45: 1610-1617.

[24] Airley R, Evans A, Mobasheri A, Hewitt SM. Glucose transporter Glut-1 is detectable in peri-necrotic regions in many human tumor types but not normal tissues: study using tissue microarrays. Ann Anat 2010; 192: 133-138.

[25] Aliaga A, Rousseau JA, Cadorette J, Croteau E, van Lier JE, Lecomte R, Bénard F. A small animal positron emission tomography study of the effect of chemotherapy and hormonal therapy on the uptake of 2-deoxy-2-[F-18]fluoro-D-glucose in murine models of breast cancer. Mol Imaging Biol 2007; 9: 144-150.

[26] Takeuchi S, Zhao S, Kuge Y, Zhao Y, Nishijima K, Hatano T, Shimizu Y, Kinoshita I, Tamaki N, Dosaka-Akita H. [18F]-fluorothymidine PET/CT as an early predictor of tumor response to treatment with cetuximab in human lung cancer xenografts. Oncol Rep 2011; 26: 725-730.

[27] Jensen MM, Erichsen KD, Björkling F, Madsen J, Jensen PB, Højgaard L, Sehested M, Kjær A. Early detection of response to experimental chemotherapeutic Top216 with [18F] FLT and [18F] FDG PET in human ovary cancer xenografts in mice. PLoS One 2010; 5: e12965.

[28] Whisenant JG, McIntyre JO, Peterson TE, Kang H, Sánchez V, Manning HC, Arteaga CL, Yankeelov TE. Utility of [18F] FLT-PET to assess treatment response in trastuzumab-resistant and trastuzumab-sensitive HER2-overexpressing human breast cancer xenografts. Mol Imaging Biol 2015; 17: 119-128.

[29] Chalkidou A, Landau DB, Odell EW, Cornelius VR, O'Doherty MJ, Marsden PK. Correlation between ki-67 immunohistochemistry and [18F]-fluorothymidine uptake in patients with cancer: a systematic review and meta-analysis. Eur J Cancer 2012; 48: 3499-3513.

[30] Sugiyama M, Sakahara H, Sato K, Harada N, Fukumoto D, Kakiuchi T, Hirano T, Kohno E, Tsukada H. Evaluation of 3'-deoxy-3'-[18F]-fluorothymidine for monitoring tumor response to radiotherapy and photodynamic therapy in mice. J Nucl Med 2004; 45: 1754-1758.

[31] Peterson LM, Mankoff DA, Lawton T, Yagle K, Schubert EK, Stekhova S, Gown A, Link JM, Tewson T, Krohn KA. Quantitative imaging of estrogen receptor expression in breast cancer with PET and [18F]-fluoroestradiol. J Nucl Med 2008; 49: 367-374.

[32] Lin FI, Gonzalez EM, Kummar S, Do K, Shih J, Adler S, Kurdziel KA, Ton A, Turkbey B, Jacobs PM, Bhattacharyya S, Chen AP, Collins JM, Doroshow JH, Choyke PL, Lindenberg ML. Utility of [18F]-fluoroestradiol (18F-FES) PET/CT imaging as a pharmacodynamic marker in patients with refractory estrogen receptor-positive solid tumors receiving Z-endoxifen therapy. Eur J Nucl Med Mol Imaging 2017; 44: 500-508.

[33] Lattrich C, Schüler S, Häring J, Skrzypczak M, Ortmann O, Treeck O. Effects of a combined treatment with tamoxifen and estrogen receptor β agonists on human breast cancer cell lines. Arch Gynecol Obstet 2014; 289: 163-17